


Article

Study on High-Temperature, Ultra-Low Wear Behaviors of Ti6Al4V Alloy with Thermal Oxidation Treatment

Qunfeng Zeng ^{1,*} , Shichuan Sun ¹, Zeming Pang ¹ and Xunkai Wei ²

¹ Key Laboratory of Education Ministry for Modern Design and Rotor-Bearing System, Xi'an Jiaotong University, Xi'an 710049, China; sunsc719@163.com (S.S.); pangzeming@stu.xjtu.edu.cn (Z.P.)

² Beijing Aeronautical Engineering Technical Research Center, Beijing 100076, China; xunkai_wei@126.com

* Correspondence: zengqf1949@gmail.com

Abstract: Thermal oxidation (TO) is a simple and economical way to enhance the wear resistance of the Ti6Al4V alloy. The TO temperature has a very important effect on the tribological properties of the TiO₂ layer formed. However, the impact of the oxidation temperature on the high-temperature tribological behavior of a TO-treated Ti6Al4V alloy is not clear. Therefore, the Ti6Al4V alloy was oxidized at 400 °C, 600 °C, and 700 °C for 36 h, and the sliding friction experiments were conducted at room temperature (RT) and 400 °C with a Si₃N₄ ball as the counter body to comparatively study the effect of the oxidation temperature on the high-temperature friction behavior of the TO-treated Ti6Al4V alloy. The results show that the TO treatment can effectively improve the wear resistance of the samples at both room and high temperatures. Among them, the oxidation-treated samples at 700 °C show the best wear resistance, with a reduction of 92.6% at high temperatures; the amount of wear loss at room temperature was so small that it was almost incalculable. At room temperature, the friction surface formed uneven agglomerate formations, resulting in an elevated coefficient of friction (CoF) compared to the untreated samples. At a high temperature, however, the CoF is reduced compared to the untreated samples due to the formation of a homogeneous transfer film in the wear area that is caused by the interaction of Si₃N₄ and oxygen.

Keywords: Ti6Al4V; thermal oxidation; high-temperature wear behavior



Citation: Zeng, Q.; Sun, S.; Pang, Z.; Wei, X. Study on High-Temperature, Ultra-Low Wear Behaviors of Ti6Al4V Alloy with Thermal Oxidation Treatment. *Coatings* **2024**, *14*, 416. <https://doi.org/10.3390/coatings14040416>

Academic Editors: Maria Vittoria Diamanti and Ludmila B. Boinovich

Received: 22 February 2024

Revised: 27 March 2024

Accepted: 29 March 2024

Published: 31 March 2024



Copyright: © 2024 by the authors. Licensee MDPI, Basel, Switzerland. This article is an open access article distributed under the terms and conditions of the Creative Commons Attribution (CC BY) license (<https://creativecommons.org/licenses/by/4.0/>).

1. Introduction

The Ti6Al4V alloy, due to its low density, high specific strength, and excellent performance, is one of the mainstream materials used for making aero-engine blades [1–5]. In an aero engine, the clearance between the blade case is a key factor that affects its efficiency [6–8]. In order to minimize the clearance, the casing is coated with a sacrificial abradable seal [9–12]. During engine operation, the blade tip and the sealing coating are subject to high-speed scraping. Therefore, improving the wear resistance of Ti6Al4V alloy blade tips is crucial for the safety and lifetime of aero engines. For a Ti6Al4V alloy, thermal oxidation (TO) is a simple and efficient means to enhance its wear resistance due to the high affinity of titanium for oxygen and the high hardness of titanium dioxide [13–16].

Guleryuz and Cimenoglu [17] investigated the effect of the TO process on the room temperature dry sliding wear behavior of a Ti6Al4V alloy treated at 600 °C for 60 h. The TO process induced a hard surface layer of TiO₂ and an oxygen diffusion zone, which improved the surface hardness from 450 to 1300 HV_{0.01} and improved the wear resistance. Wang et al. [18] performed thermal oxidation at 600 °C to 800 °C for 4 h under a vapor environment and investigated the room temperature tribological properties. It was found that the optimal oxidation temperature was 700 °C, with an 80% reduction in the wear volume. Then, they studied the effects of different durations from 2 h to 8 h under a water-oxidizing atmosphere [19]. The results showed that the growth of the oxide gradually became sufficient with the increase in time, and when the time was more than 6 h, the oxide particles were overgrown, and the surface was gradually roughened.

However, most of the available studies have focused on the effect of the thermal oxidation technique on the room temperature tribological properties of the samples, and little research has been conducted on the wear behavior of a thermally oxidized Ti6Al4V alloy at elevated temperatures [20,21]. The existing literature shows that the thermal oxidation temperature has a significant effect on the wear resistance of the Ti6Al4V alloy, but there are few studies on its role on the friction and wear properties at high temperatures [22,23]. In fact, the operating temperature of Ti6Al4V alloy blades can reach up to 400 °C [24,25]. For titanium and its alloys, the oxide layer (OL) and the oxidation diffusion zone (ODZ) form simultaneously at temperatures above 400 °C. The OL and ODZ form at the same time. However, at temperatures above 800 °C, the thick OL and the ODZ detach, leading to a reduction in the high-temperature properties of the alloy [21,26,27]. Therefore, in this investigation, the Ti6Al4V alloy was oxidized at three different temperatures of 400 °C (TO-400 °C), 600 °C (TO-600 °C), and 700 °C (TO-700 °C) for 36 h. Sliding wear experiments were conducted at room temperature and 400 °C to comparatively study the effect of the thermal oxidation temperature on the high-temperature tribological performance of a Ti6Al4V alloy.

2. Experimental Section

2.1. Materials and Thermal Oxidation

The components of the Ti6Al4V alloy were 5.85 wt% Al, 3.68 wt% V, 0.18 wt% O, 1.3 wt% N, 1.47 wt% Fe, and Ti was balanced. First, the Ti6Al4V alloy was cut into round blocks with a diameter of 30 mm and a thickness of 3 mm for use as the experimental samples. Before thermal oxidation, one side of the samples was polished to Ra 0.02 µm, which was measured using a laser scanning confocal microscope (LSCM, OLS4000, Japan), and then cleaned with anhydrous ethanol. The polished samples were heated at 400 °C, 600 °C, and 700 °C for 36 h using a tube furnace, and then the furnace cooled to room temperature.

2.2. Characterization

The oxide phases formed after TO were analyzed using X-ray diffractometry (Bruker D8 ADVANC, Saarbrücken, Germany), using a Cu-targeted source at a wave length of 0.15418 nm. The oxidized samples were scanned from 20° to 90° (2θ), using a step size of 0.02° /s and an acquisition time of 0.05 s at each the step. The hardness measurements were carried out at three different locations on the oxide surface with a Vickers hardness tester (TMVS-1, Beijing, China), at a load of 50 g and a hold time of 15 s, following the ISO standard 6507 [28]. Field emission scanning electron microscopy (FE-SEM) (GeminiSEM 500, Zeiss, German) was used to evaluate the surface morphologies as well as the microstructures of the abrasive marks after oxidation, and energy dispersive spectroscopy (EDS) was used to analyze the elemental composition of the surface. The surface of the wear tracks was scanned using a laser scanning confocal microscope (LSCM, OLS4000, Japan) to measure the cross-sectional area of the abrasion marks and calculate the wear rate.

2.3. Tribological Testing

Both the room temperature and high-temperature friction experiments were carried out using an RTEC Multi-Function Friction Tester in a ball-on-disc friction mode following the ASTM standard G99 [29]. The friction occurred in the form of a rotational motion in an air atmosphere. A silicon nitride ceramic (Si₃N₄) ball with a diameter of 9.525 mm was used as the friction partner. The load was a constant load of 3 N. The relative sliding speed between the ball and the disk was 0.05 m/s for a duration of 1800 s. The experiments were carried out at room temperature and 400 °C, respectively.

3. Results and Discussion

3.1. Oxide Layer

Figure 1 shows the SEM images of the Ti6Al4V alloy after TO treatment at different temperatures. The thickness of the oxide layer gradually increases with the increase in temperature. Traces left by polishing can still be clearly seen in the samples after TO treatment at 400 °C, the abrasion marks observed in the samples after treatment at 600 °C are significantly reduced, and the traces of polishing can no longer be observed at all on the surface after treatment at 700 °C. As the TO temperature increases, the surface unevenness of the samples increases significantly.

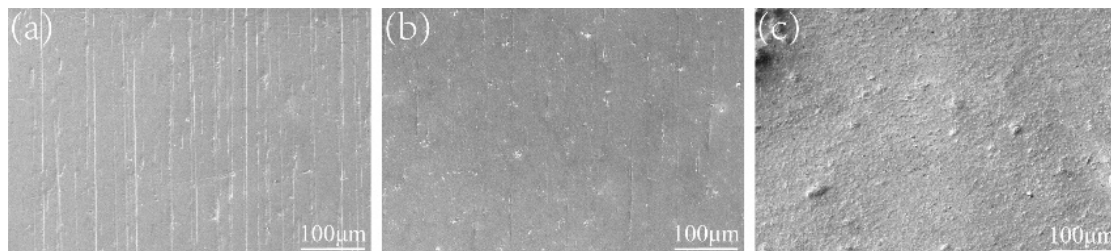


Figure 1. SEM morphology of oxide layers obtained at (a) 400 °C, (b) 600 °C, and (c) 700 °C.

Figure 2 shows the cross-sectional images of the oxide layers in TO-treated samples. When the oxidation temperature is 400 °C, it can be observed that a significant oxygen diffusion occurs, but the degree of oxidation is weak, the oxides do not gather to form a complete oxide layer, and there is no obvious demarcation line with the substrate. However, in Figure 2a, clear agglomeration can be observed, and it becomes denser the closer to the surface it occurs. In the process of oxide formation, the alloy first adsorbs oxygen molecules in the atmosphere, then the oxide nucleates and gradually aggregates to form an oxide film [18,30]. The oxide on the surface of the 400 °C TO sample is on the verge of forming an oxide film, and the oxide aggregation is obvious. As the temperature rises, the rate of oxide generation accelerates and the oxide grows and agglomerates, forming complete oxide layers [31]. As shown in Figure 2b,c, clear oxide layers can be observed in 600 °C and 700 °C TO samples, where the oxide layer thickness of the 700 °C TO sample reaches 3.656 μm.

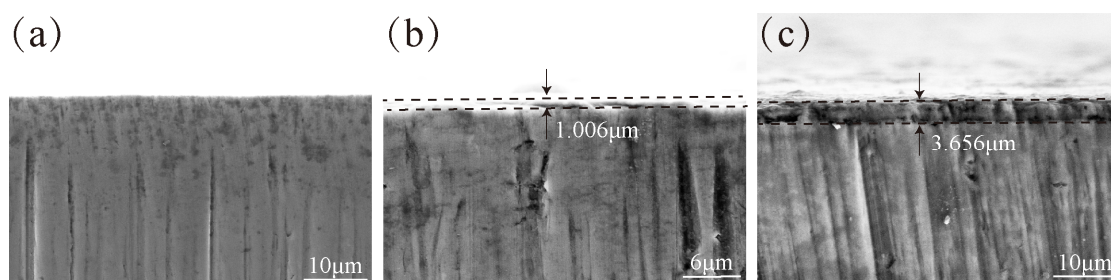


Figure 2. Cross-sectional images of oxide layers obtained at (a) 400 °C, (b) 600 °C, and (c) 700 °C.

Figure 3 shows the XRD patterns of the untreated samples and the TO-treated samples at different temperatures. The sample oxidized at 400 °C did not show TiO₂ phase peaks due to the thin oxide layer at this time [21]. The sample oxidized at 600 °C started to show TiO₂ phase peaks, but with a low peak intensity. The sample oxidized at 700 °C had a clear rutile-TiO₂ phase peak with a stronger peak intensity. Table 1 shows the microhardness values of TO-treated samples and the surface element content obtained using EDS. The microhardness of the samples gradually increased with an increasing TO treatment temperature. The greatest increase in hardness was observed for the samples treated at 700 °C, from 370 ± 20 HV_{0.05} to 1250 ± 40 HV_{0.05}. In order to obtain the intrinsic

hardness of the oxide layer, the hardness of the oxide layer was calculated using the Jonsson and Hogmark model [32]:

$$H_f = H_s + \frac{H_c - H_s}{2Ct/h - C^2(t/h)^2} \tag{1}$$

where H_f is the hardness of the coatings, H_s is the hardness of the substrate, H_c is the composite hardness, C is a constant dependent upon the indenter geometry, t is the coating thickness, and h is the indentation depth. According to Equation (1), the intrinsic hardness of the 600 °C and 700 °C TO samples can be calculated as 1258.11 HV_{0.05} and 1469.51 HV_{0.05}, respectively. The intrinsic hardness of the 400 °C TO sample cannot be calculated due to an obvious demarcation line in the substrate. It can be seen that the intrinsic hardness of the oxide layer also increases with temperature. To highlight the proportionality between Ti and O, the sum of the Ti and O content was calculated as 100%. From the analysis results of EDS, it can be seen that with an increase in the oxidation temperature, the samples exhibited a gradual increase in the content of O, which gradually approached an atomic ratio for Ti to O of 1:2 in TiO₂. It indicated that the degree of oxidation and oxygen diffusion of the Ti6Al4V alloy surface gradually deepens with the increase in oxidation temperature.

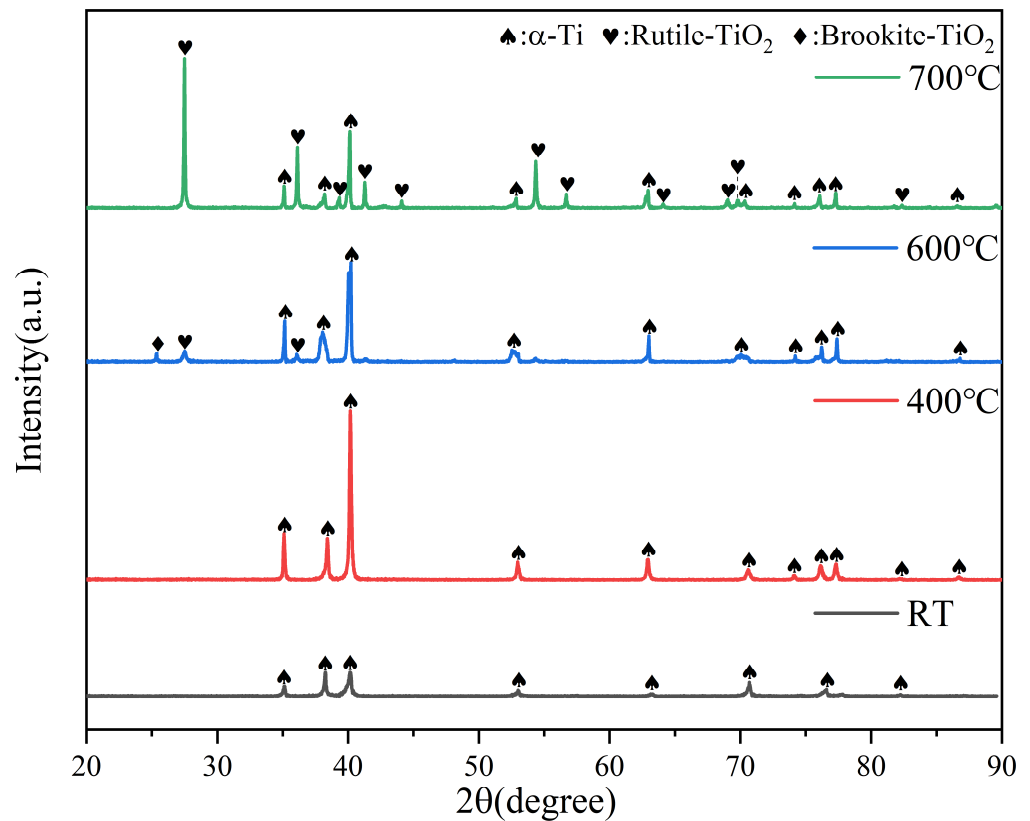


Figure 3. XRD patterns of untreated and TO-treated samples oxidized at different temperatures.

Table 1. EDS analysis of TO-treated samples at different temperatures.

Samples	Treatment Temperature (°C)	Treatment Duration (h)	Hardness (HV _{0.05})	Element Content	
				Ti (at%)	O (at%)
Untreated	-	-	366 ± 20	99.79	0.21
400 °C TO	400 °C	36 h	530 ± 20	67.02	32.98
600 °C TO	600 °C	36 h	951 ± 30	37.85	62.15
700 °C TO	700 °C	36 h	1246 ± 40	32.08	67.02

3.2. Tribological Behavior

Figure 4 shows the coefficients of friction (CoFs) of untreated and TO-treated samples tested against a Si_3N_4 ball counter body at a constant load of 3 N at room temperature (RT) and 400 °C. As shown in Figure 4a,c, the TO-treated samples show higher CoF values than untreated samples at RT. The lowest CoF (0.31) was found for the untreated sample, and the highest CoF (0.50) was found for the 600 °C TO sample, while the CoF values of the untreated sample showed a greater fluctuation. At 400 °C, the TO-treated samples exhibited a lower CoF in the stabilization phase than the untreated sample. The untreated samples had the highest CoF (0.46), and the 400 °C TO samples had the lowest CoF (0.34).

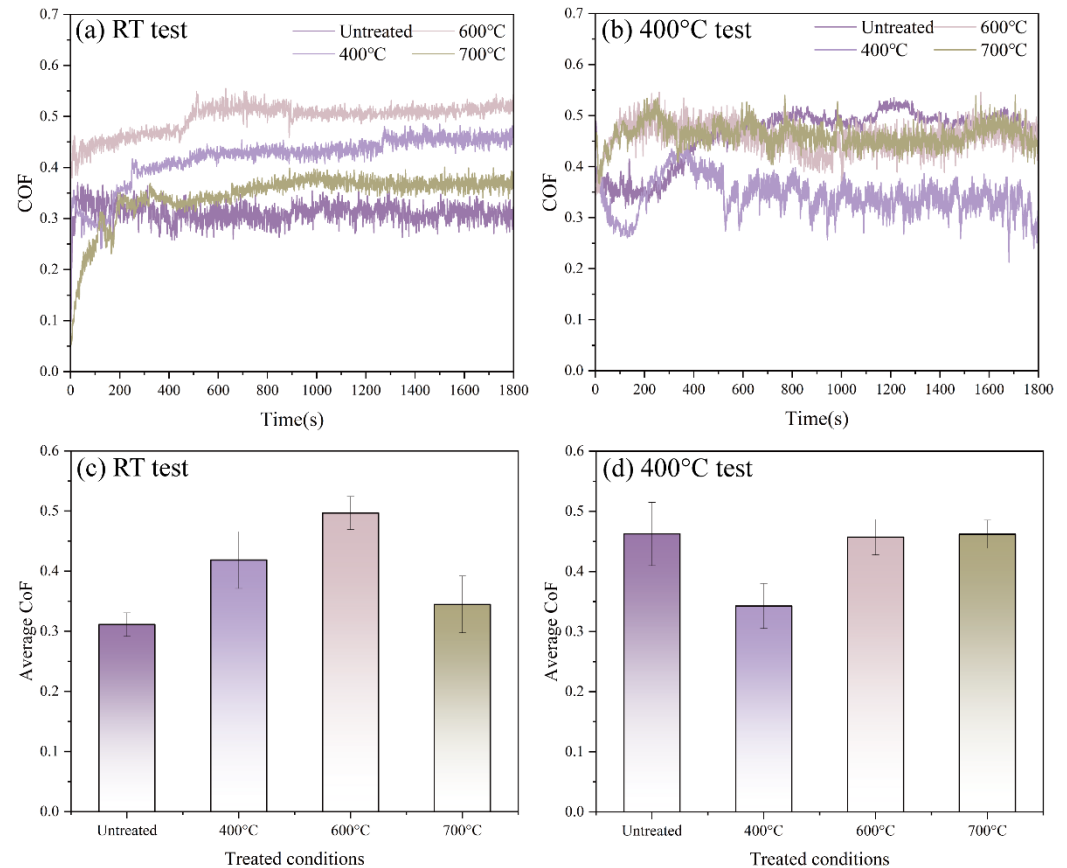


Figure 4. CoF and average CoF of untreated and TO-treated samples tested at (a,c) room temperature (RT) and (b,d) 400 °C.

Figure 5 shows the wear rates of untreated and TO-treated samples. It can be found that the TO-treated samples show excellent wear resistance, which can effectively reduce the wear rate. The low wear rate of the TO-treated samples can be attributed to the fact that the high hardness of the oxide layer improves the wear resistance of the sample's surface, reduces the stresses at the contact interface, and decreases the elastic and plastic deformation at the contact interface, which ultimately leads to a reduction in the wear. The 700 °C TO sample exhibits the best wear resistance, with a 92.6% reduction in the wear rate from $2.77 \times 10^{-4} \text{ mm}^3\text{N}^{-1}\text{m}^{-1}$ to $2.05 \times 10^{-5} \text{ mm}^3\text{N}^{-1}\text{m}^{-1}$ at 400 °C, while at RT, its wear is so small, it is almost incalculable. This also proves that the high surface hardness resulting from the formation of the oxide layer significantly increases the resistance to wear. The wear rate of the untreated sample at RT ($7.06 \times 10^{-4} \text{ mm}^3\text{N}^{-1}\text{m}^{-1}$) is higher than that at 400 °C, which may be due to the fact that the TiO_2 formed during the friction of the Ti6Al4V alloy at a high temperature formed a friction layer in the wear area, which has a certain protective effect on the samples [32]. In particular, unlike the 400 °C and 700 °C TO samples,

the 600 °C TO sample has a significantly higher wear rate at RT ($1.93 \times 10^{-4} \text{ mm}^3\text{N}^{-1}\text{m}^{-1}$) than at 400 °C ($3.01 \times 10^{-5} \text{ mm}^3\text{N}^{-1}\text{m}^{-1}$).

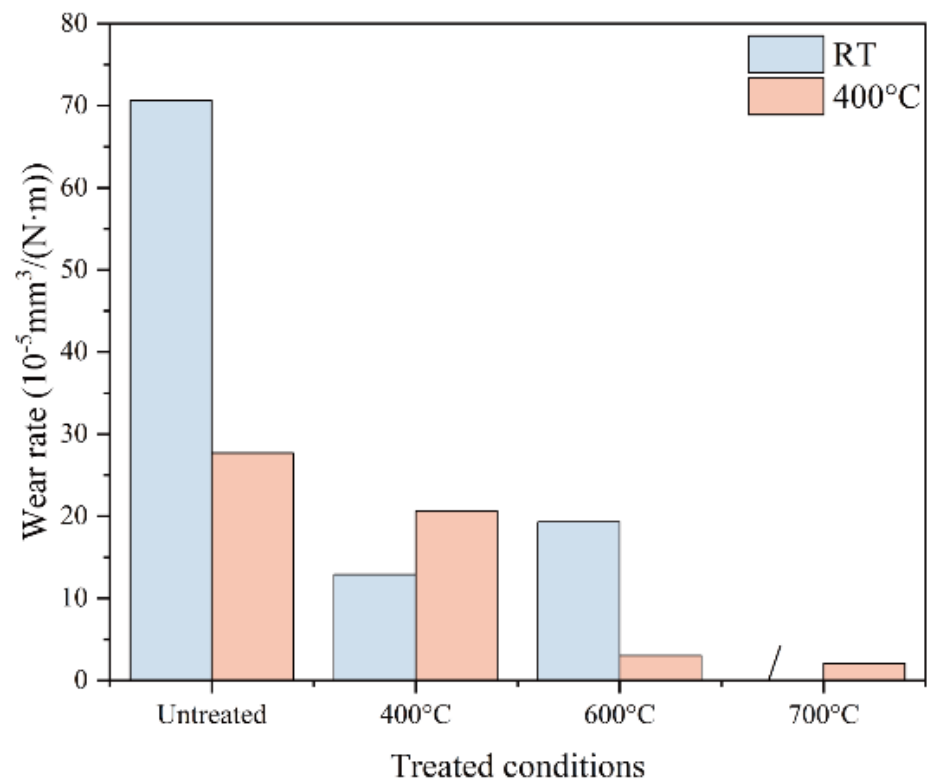


Figure 5. Wear rates of untreated and TO-treated samples tested at two temperatures.

Figure 6 shows the SEM morphology of the wear track and the element distribution of the untreated sample and TO-treated samples tested at RT. It was found that the surface of the untreated sample had a lot of wear debris distributed on it. The 400 °C and 600 °C TO surfaces show significant adhesive wear and furrow wear, while the 700 °C TO surface shows even more severe adhesive wear, with scaly adhesive layers on the surface. In addition, from the elemental distribution results, it can be seen that the wear traces of the TO-treated samples showed a significant Si diffusion phenomenon. This is due to the weak resistance of Si_3N_4 to chemical attack by atoms of the Ti6Al4V alloy, and the chemical activity of the Si element was motivated during the friction with the Ti6Al4V alloy under atmospheric conditions [33]. The diffusion of Si elements and their reaction with oxygen to form Si–O compounds leads to the increased adhesive wear at RT friction and the formation of an inhomogeneous adhesion layer. This may be one of the main reasons for the increase in the CoF. The wear track of the 400 °C and 600 °C TO samples show deep ploughing grooves due to the hard oxide layer and Si_3N_4 balls breaking up during friction and forming hard wear particles. The further aggravation of Si diffusion and ultra-high surface hardness of the 700 °C TO sample lead to no obvious ploughing grooves appearing in the wear tracks.

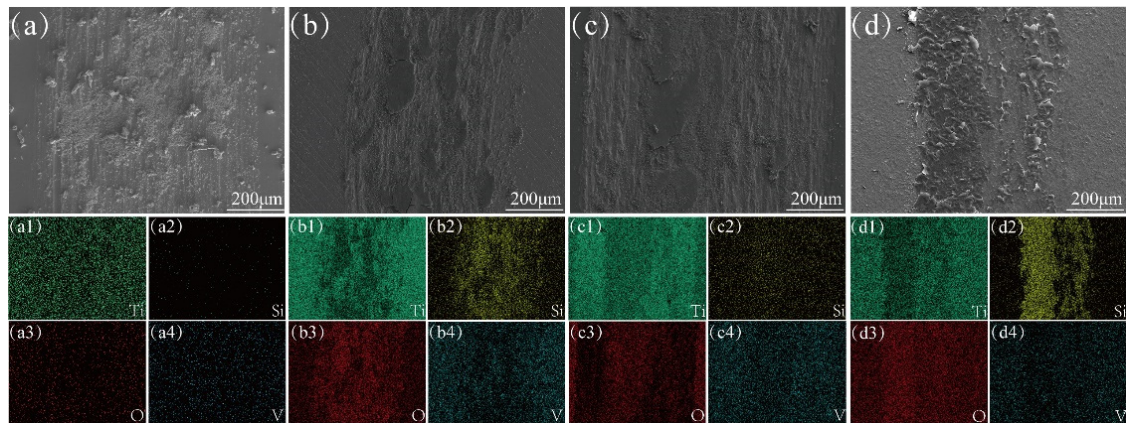


Figure 6. The SEM morphology of the wear track of the (a) untreated sample and (b) 400 °C, (c) 600 °C, and (d) 700 °C TO samples tested at RT. (a1–a4) The distribution of elements in (a). (b1–b4) The distribution of elements in (b). (c1–c4) The distribution of elements in (c). (d1–d4) The distribution of elements in (d). 1–4 are the distributions of Ti, Si, O, and V, respectively.

Figure 7 shows the SEM morphology of the wear track and the element distribution of the untreated sample and TO-treated samples tested at RT. From Figure 6a and its element distributions, the Si diffusion of the untreated sample was increased and significant adhesive wear was observed on the surface, which may be due to the further activation of the chemical activity of Si at a high temperature. It was found that Si diffusion of the 400 °C TO sample was significantly weakened. The thinner oxide layer on the surface of the 400 °C TO sample breaks down during friction with the hard Si_3N_4 and works together with the TiO_2 formed by the oxidation of the substrate at the high temperature, preventing the diffusion of Si. This is also the reason why the CoF of the 400 °C TO sample is lower than that of the three other samples at 400 °C [34]. The wear tracks of the 600 °C and 700 °C TO samples form a dense and uniform adhesive layer that protects the substrate, which explains their low wear rate and large fluctuations in the CoF compared to the untreated and 400 °C TO samples.

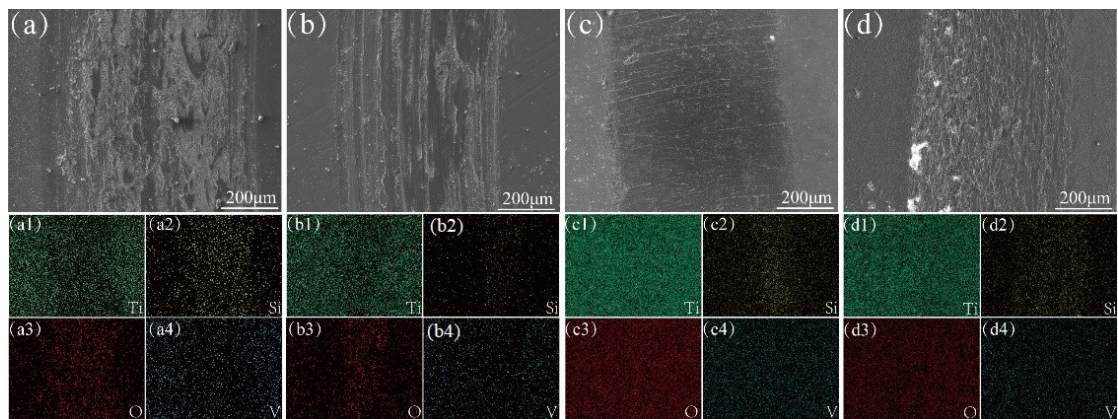


Figure 7. The SEM morphology of the wear track of the (a) untreated sample and (b) 400 °C, (c) 600 °C, and (d) 700 °C TO samples tested at 400 °C. (a1–a4) The distribution of elements in (a). (b1–b4) The distribution of elements in (b). (c1–c4) The distribution of elements in (c). (d1–d4) The distribution of elements in (d). 1–4 are the distributions of Ti, Si, O, and V, respectively.

The wear scars on the Si_3N_4 counter body tested against untreated and TO-treated samples are shown in Figure 8. At RT and 400 °C, for untreated and 400 °C TO samples, the occurrence of adhesive wear is evidenced by a very high amount of adhesion on the Si_3N_4 counter body, which is consistent with the results observed on the Ti6Al4V alloy samples' wear tracks. For the 600 °C TO samples, more adhesion on the surface of the

Si_3N_4 ball in the RT experiment corresponds to the more severe adhesive wear and higher wear rate at RT. We observed a very significant loss on the surface of the Si_3N_4 counter body against the 700 °C TO samples at RT, and there is almost no transfer on the surface, which confirms the incalculable wear rate at RT. Relatively speaking, the increase in the surface transfer of the Si_3N_4 counter body at 400 °C confirms the adhesion observed on the 700 °C TO sample surface.

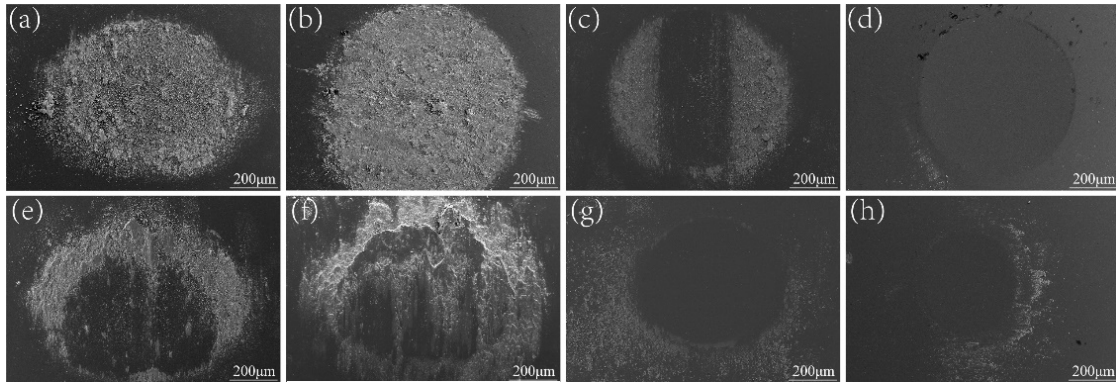


Figure 8. The SEM morphology of Si_3N_4 counter bodies tested against untreated and TO-treated samples at RT (a–d) and 400 °C (e–h): (a,e) Untreated, (b,f) 400 °C TO, (c,g) 600 °C TO, and (d,h) 700 °C TO.

3.3. Discussion

Figure 9 shows the schematic diagram of oxide layer formation and the wear mechanism. The thermal oxidation process of the Ti6Al4V alloy begins with the adsorption of oxygen molecules from the atmosphere, followed by the nucleation of the oxide, gradual agglomeration of the oxide particles to form a thin oxide film, and finally, the formation of a thicker oxide layer with the time increase [18,30]. As the temperature rises, the oxidation reaction is catalyzed, and the rate of oxidation accelerates. In the end, the thickest oxide layer was obtained for the 700 °C TO sample in the same period of time, and the oxide layer did not show any cracking and was well bound to the substrate. The formation of a TiO_2 layer greatly improves the surface hardness of the Ti6Al4V alloy and enhances its wear resistance. Even for the 400 °C TO samples without a complete oxide layer, the diffused oxide in the oxygen diffusion zone greatly enhances the surface hardness and increases the wear resistance.

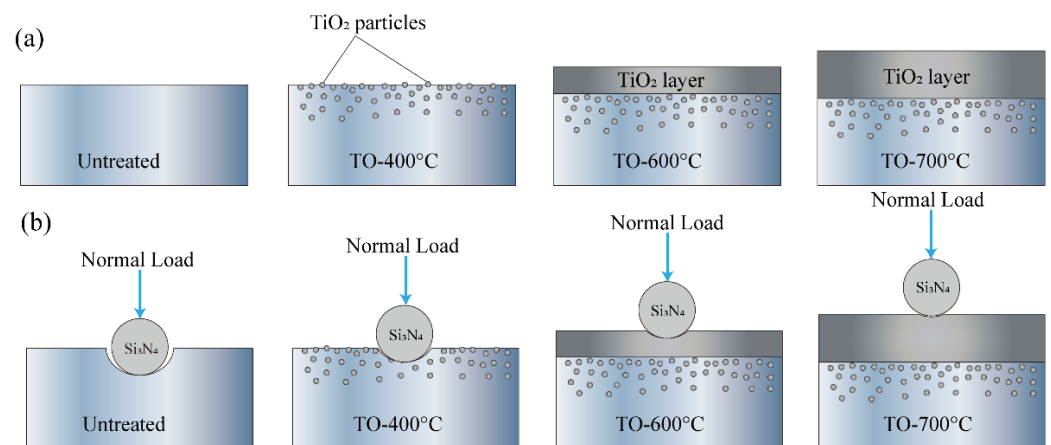


Figure 9. Schematic diagram of (a) oxide layer formation and (b) wear mechanism.

In general, thermally oxidized Ti6Al4V alloys have a high hardness due to the TiO_2 on the surface, and the hard particles generated during wear will result in a predominantly

abrasive form of wear [35]. However, when Si_3N_4 is used as the counter body, the activity of the Si in Si_3N_4 is activated, resulting in Si diffusion during friction and severe adhesive wear. In particular, adhesive wear was most severe for the 700 °C TO sample, which had the best wear resistance, with almost unidirectional material transfer from the Si_3N_4 ball to the 700 °C TO sample. A continuous transfer film was formed on the surface of the 700 °C TO sample, whereas material removal from the surface of the silicon nitride ball was evident, and there was little adhesion. The formation of a transfer film further protects the sample from wear, ultimately leading to the low wear rate of the 700 °C TO sample.

At 400 °C, the increase in temperature further stimulates the chemical activity of the Si in the Si_3N_4 counter body, leading to a further increase in adhesive wear. This is why the CoF curves of the TO-treated samples fluctuate even more. At high temperatures, hard counter bodies tend to cause fractures in the titanium dioxide oxide layer during friction with the oxide layer [36]. However, when Si_3N_4 is used as a counter body, the increased adhesive wear due to Si diffusion instead protects the oxide layer from fracture, which allows the oxide layer to maintain a good bond strength with the substrate after a period of friction. This implies that when a TO-treated Ti6Al4V alloy is used as a friction partner with Si_3N_4 , the anti-wear properties of the oxide layer may be able to be maintained for a longer period of time. Especially for the 600 °C and 700 °C TO samples, which have better hardness and wear resistance, the fine and uniform friction layer formed at the wear tracks can better protect the oxide layer from further wear.

4. Conclusions

The effect of the thermal oxidation temperature on the tribological performance of the Ti6Al4V alloy was investigated systemically. The results show that a suitable thermal oxidation temperature can effectively enhance the anti-wear performance of the Ti6Al4V alloy. The conclusions obtained from the present work can be summarized as follows:

- (1) The thermal oxidation temperature has a considerable influence on the formation of the oxide layer. As the temperature increases, the oxide grows and agglomerates to form a complete oxide layer with an increasing thickness. The sample treated at 700 °C has the highest thickness (3.656 μm) and the surface hardness increases from $366 \pm 20 \text{ HV}_{0.05}$ to $1246 \pm 40 \text{ HV}_{0.05}$.
- (2) The TiO_2 layer formed by thermal oxidation can significantly enhance the wear resistance of the Ti6Al4V alloy. The oxidation-treated samples at 700 °C show the best wear resistance, with a reduction of 92.6% at high temperatures, and the amount of wear at room temperature is almost incalculable.
- (3) The wear mechanism at RT and 400 °C is adhesive wear. In addition, due to the activation of the tribochemical activity of Si during the friction of Si_3N_4 with the Ti6Al4V alloy, there is clear silicon diffusion in the wear track.

Author Contributions: Resources, Z.P.; Data curation, S.S. and Z.P.; Writing—original draft, Q.Z.; Writing—review & editing, S.S.; Supervision, X.W.; Funding acquisition, Q.Z. and X.W. All authors have read and agreed to the published version of the manuscript.

Funding: The present work was financially supported by National Science and Technology Major Project (j2019-IV-0004-0071), Shanxi Province Science and Technology Cooperation and Exchange Special Project (202204041101021), and Liaoning Key Laboratory of Aero-Engine Materials Tribology (LKLAMTF202401).

Institutional Review Board Statement: Not applicable.

Informed Consent Statement: Not applicable.

Data Availability Statement: Data are contained within the article.

Conflicts of Interest: The authors declare no conflict of interest.

References

1. Pavlenko, D.; Dvirnyk, Y.; Przysowa, R. Advanced materials and technologies for compressor blades of small turbofan engines. *IOP Conf. Ser. Mater. Sci. Eng.* **2021**, *1024*, 012061. [[CrossRef](#)]
2. Zeng, Q.; Wang, Z.; He, W.; Pang, Z.; Ning, Z.; Chen, R.; Zheng, C.; Yan, C.; Guo, L. Improved tribocorrosion properties of Ti₆Al₄V alloy by anodic plasma electrolytic oxidation. *Adv. Eng. Mater.* **2023**, *25*, 2300228. [[CrossRef](#)]
3. Yang, W.; He, X.; Li, H.; Dong, J.; Chen, W.; Xin, H.; Jin, Z. A tribological investigation of SLM fabricated TC₄ Titanium alloy with carburization pre-treatment. *Ceram. Int.* **2020**, *46*, 3043–3050. [[CrossRef](#)]
4. Zhu, Y.; Chen, X.; Zou, J.; Yang, H. Sliding wear of selective laser melting processed Ti₆Al₄V under boundary lubrication conditions. *Wear* **2016**, *368–369*, 485–495. [[CrossRef](#)]
5. Shao, M.; Wang, W.; Yang, H.; Zhang, X.; He, X. Preparation of wear-resistant coating on Ti₆Al₄V alloy by cold spraying and plasma electrolytic oxidation. *Coatings* **2021**, *11*, 1288. [[CrossRef](#)]
6. Xue, W.; Gao, S.; Duan, D.; Wang, L.; Liu, Y.; Li, S. Study on the high-speed rubbing wear behavior between Ti₆Al₄V blade and nickel-graphite abradable seal Coating. *J. Tribol.* **2017**, *139*, 021604. [[CrossRef](#)]
7. Xue, W.; Gao, S.; Duan, D.; Liu, Y.; Li, S. Material transfer behaviour between a Ti₆Al₄V blade and an Aluminum hexagonal boron nitride abradable coating during high-speed rubbing. *Wear* **2015**, *322–323*, 76–90. [[CrossRef](#)]
8. Tüfekci, M. Performance Evaluation Analysis of Ti-6Al-4V foam fan blades in aircraft engines: A numerical study. *Compos. Part C Open Access* **2023**, *12*, 100414. [[CrossRef](#)]
9. Zeng, Q.; Qi, W. High temperature superlubricity behaviors achieved by AlSiN coatings against WS₂ coatings at 600 °C. *Ceram. Int.* **2024**, *50*, 3787–3796. [[CrossRef](#)]
10. Zeng, Q. High-temperature superlubricity performance of h-BN coating on the textured Inconel X750 Alloy. *Lubricants* **2023**, *11*, 258. [[CrossRef](#)]
11. Baiz, S.; Fabis, J.; Boidin, X.; Desplanques, Y. Experimental investigation of the blade/seal interaction. *Proc. Inst. Mech. Eng. Part J* **2013**, *227*, 980–995. [[CrossRef](#)]
12. Scrinzi, E.; Giovannetti, I.; Sheng, N.; Leblanc, L. *Development of New Abradable/Abrasive Sealing Systems for Clearance Control in Gas Turbines*; American Society of Mechanical Engineers Digital Collection; ASME: Hamburg, Germany, 2014.
13. Philip, J.; Mathew, J.; Kuriachen, B. Tribology of Ti₆Al₄V: A review. *Friction* **2019**, *7*, 497–536. [[CrossRef](#)]
14. Borgioli, F.; Galvanetto, E.; Iozzelli, F.; Pradelli, G. Improvement of wear resistance of Ti-6Al-4V alloy by means of thermal oxidation. *Mater. Lett.* **2005**, *59*, 2159–2162. [[CrossRef](#)]
15. Dong, H.; Bell, T. Enhanced wear resistance of Titanium surfaces by a new thermal oxidation treatment. *Wear* **2000**, *238*, 131–137. [[CrossRef](#)]
16. Zeng, Q.; Zhang, W. A systematic review of the recent advances in superlubricity research. *Coatings* **2023**, *13*, 1989. [[CrossRef](#)]
17. Guleryuz, H.; Cimenoglu, H. Surface modification of a Ti-6Al-4V alloy by thermal oxidation. *Surf. Coat. Technol.* **2005**, *192*, 164–170. [[CrossRef](#)]
18. Wang, S.; Liao, Z.; Liu, Y.; Liu, W. Influence of thermal oxidation temperature on the microstructural and tribological behavior of Ti₆Al₄V Alloy. *Surf. Coat. Technol.* **2014**, *240*, 470–477. [[CrossRef](#)]
19. Wang, S.; Liao, Z.; Liu, Y.; Liu, W. Influence of thermal oxidation duration on the microstructure and fretting wear behavior of Ti₆Al₄V alloy. *Mater. Chem. Phys.* **2015**, *159*, 139–151. [[CrossRef](#)]
20. Lou, M.; Alpas, A. High temperature wear mechanisms in thermally oxidized Titanium alloys for engine valve applications. *Wear* **2019**, *426–427*, 443–453. [[CrossRef](#)]
21. Liu, J.; Suslov, S.; Lim, S.; Qin, H.; Ren, Z.; Ma, C.; Wang, G.; Doll, G.; Cong, H.; Dong, Y.; et al. Effects of ultrasonic nanocrystal surface modification on the thermal oxidation behavior of Ti₆Al₄V. *Surf. Coat. Technol.* **2017**, *325*, 289–298. [[CrossRef](#)]
22. Yuan, S.; Lin, N.; Zou, J.; Lin, X.; Liu, Z.; Yu, Y.; Wang, Z.; Zeng, Q.; Chen, W.; Tian, L.; et al. In-situ fabrication of gradient titanium oxide ceramic coating on laser surface textured Ti6Al4V alloy with improved mechanical property and wear performance. *Vacuum* **2020**, *176*, 109327. [[CrossRef](#)]
23. Zhang, C.; Li, C.; Zhang, J. Study on effect of thermal oxidation treatment on wear resistance of Titanium alloy. *Surf. Technol.* **2008**, *37*, 18–20 + 23.
24. Li, Y.; Zhao, Y.; Zeng, W. Application and development of aerial Titanium alloys. *Mater. Rep.* **2020**, *34*, 280–282.
25. Singh, P.; Pungotra, H.; Kalsi, N. On the characteristics of Titanium alloys for the aircraft applications. *Mater. Today Proc.* **2017**, *4*, 8971–8982. [[CrossRef](#)]
26. Guleryuz, H.; Cimenoglu, H. Oxidation of Ti-6Al-4V Alloy. *J. Alloys Compd.* **2009**, *472*, 241–246. [[CrossRef](#)]
27. Kumar, S.; Sankara Narayanan, T.; Ganesh Sundara Raman, S.; Seshadri, S. Thermal Oxidation of Ti₆Al₄V alloy: Microstructural and electrochemical characterization Ti₆Al₄V. *Mater. Chem. Phys.* **2010**, *119*, 337–346. [[CrossRef](#)]
28. *ISO 6507*; Metallic Materials-Vickers Hardness Test—Part 1: Test Method. International Organization for Standardization: Geneva, Switzerland, 2023.
29. *ASTM G99-23*; Standard Test Method for Wear Testing with a Pin-on-Disk Apparatus. American Society for Testing and Materials: West Conshohocken, PA, USA, 2023.
30. Krzysztof, A. The influence of thermal oxidation parameters on the growth of oxide layers on titanium. *Vacuum* **2017**, *144*, 94–100.
31. Zeng, Q.; Ning, Z.; Pang, Z.; Wang, Z.; Zheng, C. Self-assembled multilayer WS₂/GO films on amorphous silicon coating for enhancing the lubricating properties. *Appl. Surf. Sci.* **2023**, *624*, 157184. [[CrossRef](#)]

32. Jönsson, B.; Hogmark, S. Hardness Measurements of Thin Films. *Thin Solid Films* **1984**, *114*, 257–269. [[CrossRef](#)]
33. Alvi, S.; Neikter, M.; Antti, M.; Akhtar, F. Tribological performance of Ti₆Al₄V at elevated temperatures fabricated by electron beam powder bed fusion. *Tribol. Int.* **2021**, *153*, 106658. [[CrossRef](#)]
34. Dang, J.; Zhang, H.; Ming, W.; An, Q.; Chen, M. New observations on wear characteristics of solid Al₂O₃/Si₃N₄ceramictool in high speed milling of additive manufactured Ti₆Al₄V. *Ceram. Int.* **2020**, *46*, 5876–5886. [[CrossRef](#)]
35. Sun, Q.; Hu, T.; Fan, H.; Zhang, Y.; Hu, L. Thermal Oxidation Behavior and Tribological Properties of Textured TC₄ Surface: Influence of Thermal Oxidation Temperature and Time. *Tribol. Int.* **2016**, *94*, 479–489. [[CrossRef](#)]
36. Singh, K.; Raman, S. High temperature sliding wear behaviour of Ti₆Al₄V thermal oxidised for different oxidation durations. *Met. Mater. Int.* **2023**, *29*, 357–368. [[CrossRef](#)]

Disclaimer/Publisher’s Note: The statements, opinions and data contained in all publications are solely those of the individual author(s) and contributor(s) and not of MDPI and/or the editor(s). MDPI and/or the editor(s) disclaim responsibility for any injury to people or property resulting from any ideas, methods, instructions or products referred to in the content.